Engineered microsphere contrast agents for optical coherence tomography

Tin Man Lee, Amy L. Oldenburg, Shoeb Sitafalwalla, Daniel L. Marks, and Wei Luo

Beckman Institute for Advanced Science and Technology, University of Illinois at Urbana—Champaign, Urbana, Illinois 61801

Farah Jean-Jacques Toublan and Kenneth S. Suslick

Department of Chemistry, University of Illinois at Urbana—Champaign, Urbana, Illinois 61801

Stephen A. Boppart

Department of Electrical and Computer Engineering, Bioengineering Program, Beckman Institute for Advanced Science and Technology, College of Medicine, 405 North Mathews Avenue, University of Illinois at Urbana—Champaign, Urbana, Illinois 61801

Received February 10, 2003

Contrast agents are utilized in virtually every imaging modality to enhance diagnostic capabilities. We introduce a novel class of optical contrast agent, namely, encapsulating microspheres, that are based not on fluorescence but on scattering nanoparticles within the shell or core. The agents are suitable for reflection- or scattering-based techniques such as optical coherence tomography, light microscopy, and reflectance confocal microscopy. We characterize the optical properties of gold-, melanin-, and carbon-shelled contrast agents and demonstrate enhancement of optical coherence tomography imaging after intravenous injection of such an agent into a mouse.

OCIS codes: 170.4500, 160.4760, 170.4580.

When one is imaging biological tissues, it is often desirable to enhance the signals measured from specific structures. Contrast agents that produce specific image signatures have been utilized in virtually every imaging modality, including ultrasound,[1] computed tomography,[2] magnetic resonance imaging,[3] and optical microscopy.[4] Optical coherence tomography (OCT) is an emerging imaging technology that has found application in a wide range of biological and medical applications.[5] In this Letter we characterize and demonstrate a new class of optical contrast agent suitable for reflection- or scattering-based optical imaging techniques, namely, OCT but that also includes light and reflectance confocal microscopy. These agents are biocompatible,[6] are suitable for *in vivo* use, and produce enhanced backscatter that is detectable in highly scattering tissue. These agents may be tailored to adhere to specific molecules, cells, or tissue types, and thus provide additional selectivity that can enhance the utility of OCT as an emerging diagnostic technique.

OCT is capable of cellular-resolution imaging and may ultimately have a role in the early diagnosis of human malignancies.[7] Although morphological differences between normal and neoplastic tissues can be obvious at later stages of tumor development, it is challenging to detect early-stage tumors or tumors that are morphologically (or optically) similar to surrounding normal tissue. Contrast agents have been known to increase the diagnostic and analytical capabilities of the modality by site-specifically labeling of tissues or cells of interest. This should also be true for OCT, which overcomes the limitation of relying on inherent optical properties of the tissue to provide contrast to differentiate normal from pathological tissue. Inasmuch as OCT detects scattering changes, image contrast enhancement can be achieved by delivery of highly scattering contrast agents into the tissue and allowing the agents to attach to specific regions of interest. In ultrasound and OCT, air-filled microbubbles have been used as contrast agents,[1,8] but they have not been designed to incorporate nanoparticles or materials that can enhance the optical signal. We have engineered optical contrast agents that are microspheres 0.2 to 15 μm in diameter with an approximately 50-nm-thick protein shell. The microspheres are designed to incorporate in their shells and encapsulate in their cores a wide range of nanoparticles and materials that alter the local optical properties of tissue. The protein shell may also be functionalized to target the agents to specific regions of interest.

Fabrication protocols have been developed to facilitate variation of microsphere size, shell or encapsulated materials, and surface protein features. We fabricated microspheres by sonicating with high-intensity ultrasound the interface between a 5% weight per volume solution of bovine serum albumin and a solution containing the material to be incorporated into the shell or encapsulated in the core. The high-intensity ultrasound necessary for the reaction was generated by a titanium horn with tip diameter of 1.25 cm, driven at 20 kHz. The solutions were sonicated for 3 min at an acoustic power of 76 W/cm^2. The diameter of the microspheres (0.2–15 μm) depended on the acoustic power and on the frequency of the ultrasound. Solutions of microspheres were washed with nanopure water and filtered to remove

0146-9592/03/171546-03$15.00/0

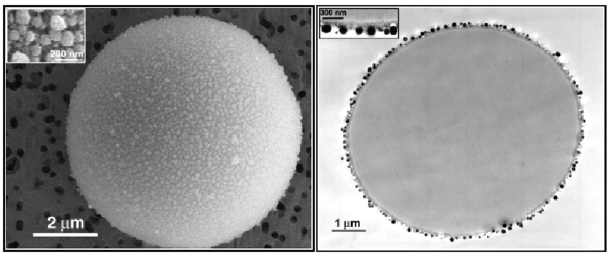

Fig. 1. Scanning- (left) and transmission- (right) electron micrographs of an oil-filled microsphere contrast agent, showing scattering silica nanoparticles in the shell.

fragments. A size range of 0.2–2 μm was selected to enable the microspheres to pass readily through the living microcirculation.

Microspheres were resuspended in nanopure water. To prevent settling during optical characterization, they were mixed and warmed liquid agarose and allowed to solidify. Average size, size distributions, and initial concentrations (average 1.1×10^{10} microspheres/mL) were determined by Coulter Multisizer II analysis of each sample. Scanning- and transmission-electron micrographs of a representative contrast agent with an oil-filled core and scattering silica nanoparticles embedded in the shell are shown in Fig. 1. The trasnmission-electron micrograph demonstrates that the shell comprises essentially a monolayer of scattering nanoparticles. For this study we investigated the optical properties of three types of contrast agent for OCT by incorporating melanin, gold, and carbon nanoparticles into the shells of oil-filled microspheres. These nanoparticles were chosen to provide a higher degree of optical scattering than does biological tissue. Comparisons are also made with oil-filled contrast agents without shell nanoparticles. The encapsulation of vegetable oil as a core material made the contrast agents more stable and robust than air-filled microbubbles, extending their lifetime in solution from 3 days to several months.

The refractive indices at 800 nm, the center wavelength of our OCT optical source, were obtained from the literature for bulk melanin, gold, and carbon (Table 1). The refractive indices of the encapsulated oil ($n = 1.47$), of the agarose gel ($n = 1.34$), and of the four types of sample were also measured by OCT. For all contrast-agent samples, refractive indices were within experimental error (5%) of the index of pure agarose because of the small fractional volume of the microspheres.

The reduced scattering coefficients of the contrast agents (average concentration, 2.8×10^9 microspheres/mL) were determined by oblique-incidence reflectometry,[11] with an 800-nm laser diode. This method was chosen to characterize thick preparations and will allow for *in situ* measurement of reduced scattering coefficients simultaneously with OCT. The oil-filled agents that contained melanin, carbon, and gold nanoparticles in their shells exhibited higher reduced scattering coefficients than microspheres without scattering nanoparticles. Upper limits of the absorption coefficients were measured for the contrast agents (average concentrations, 3.1×10^7 microspheres/mL) by a spectrophotometer (Thermo Spectronic 20). All agents exhibited low absorption coefficients, as expected for these near-infrared wavelengths. We used microsphere concentrations obtained from Coulter Multisizer II measurements and an approximate anisotropy coefficient of 0.8, based on microsphere size, to calculate scattering and absorption cross sections.

To demonstrate the effects of these contrast agents on OCT images and in tissue we performed OCT following the intravenous injection of gold-shelled contrast agents into a mouse. Our fiber-based OCT system used a Nd:YVO_4-pumped titanium:sapphire laser (Lexel Laser, Inc.) as a broad-bandwidth optical source that produced 500-mW average power and approximately 90-fs pulses with an 80-MHz repetition rate at 800-nm center wavelength. Laser output was coupled into an ultrahigh-numerical-aperture fiber (UHNA4, Thorlabs, Inc.) to broaden the light spectrally from 20 to more than 100 nm, increasing the axial resolution of our system[12] from 14 to 3 μm. The ultrahigh-numerical-aperture fiber was spliced directly to the single-mode fiber of a broadband 50:50 fiber coupler (Gould Fiber Optics). The reference arm of the OCT interferometer contained a galvanometer-driven retroreflector delay line that was scanned a distance of 3 mm at a rate of 30 Hz. The sample arm beam was focused into the tissue by a 12.5-mm-diameter, 30-mm focal-length achromatic lens to a 10-μm-diameter spot size (transverse resolution). The 6-mW beam was scanned over the tissue with a

Table 1. Optical Properties of OCT Contrast Agents[a]

Contrast Agent	Microsphere Diameter (μm)	Refractive Index	Reduced Scattering Coefficient (cm^{-1})	Absorption Coefficient (cm^{-1})	Scattering Cross Section per Sphere (cm^2)	Absorption Cross Section per Sphere (cm^2)
Oil	1.61 ± 0.72	1.47	10.8 ± 1.4	0.26 ± 0.01	2.22×10^{-8}	9.4×10^{-9}
Melanin	1.99 ± 0.99	1.66[b]	18.3 ± 3.6	0.45 ± 0.02	2.33×10^{-8}	1.0×10^{-8}
Gold	1.85 ± 0.79	0.18[c]	15.2 ± 4.1	0.69 ± 0.03	4.70×10^{-8}	3.8×10^{-8}
Carbon	1.66 ± 0.66	3.08[c]	19.9 ± 4.3	0.51 ± 0.03	3.26×10^{-8}	1.5×10^{-8}

[a]Values are mean ± standard deviation for $N = 30$ measurements.
[b]Ref. 9.
[c]Ref. 10.

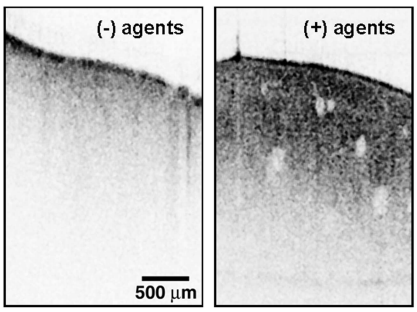

Fig. 2. OCT image enhancement with contrast agents. Images of mouse liver (left) without and (right) with gold-shelled oil-filled microsphere contrast agents.

galvanometer-controlled mirror. The envelope of the interference signal was digitized to 12-bit accuracy.

We performed OCT imaging on Swiss mice (6-week old, 27-g, males) with and without contrast agents. All animals used in this study were cared for under protocols approved by the Institutional Animal Care and Use Committee of the University of Illinois at Urbana—Champaign. Mice were anesthetized by inhalation from halothane-soaked gauze. We exposed the liver for OCT imaging by shaving the abdomen of the mouse, making a midline incision, and reflecting the abdominal skin and peritoneal wall. The liver was imaged because this is one end-organ site for collection of these contrast agents as they are broken down and cleared. A 1.3-μL volume (6.5×10^9 microsphere/mL concentration) of gold-shelled oil-filled contrast agents was injected into a tail vein. OCT of surgically exposed liver was performed 20 min after injection and following euthanasia. OCT imaging was also performed on surgically exposed liver from control mice without contrast agents. Intravenous injection is one possible route for delivering these contrast agents to living tissue. Other routes include topical administration and direct injection into a tissue site. Figure 2 shows OCT images acquired from the exposed peritoneal surface of the liver. The left-hand OCT image, acquired from a control mouse, shows little subsurface structure. A change in scattering is readily apparent in the right-hand image of Fig. 2, which was acquired following the intravenous injection of the contrast agent. More structural detail, including liver sinusoids, is shown at greater depths in the contrast-agent-enhanced liver image. We conclude, based on transmission-electron micrograph observations, that the contrast agents in the microvascular network of the liver were being phagocytosed by Kupffer cells (macrophages) and broken down.

In summary, we have engineered, characterized, and demonstrated the use of a novel class of optical contrast agent. Although we have shown the suitability of these agents for OCT, they may be broadly applicable for other reflectance- and scattering-based techniques such as light and reflectance confocal microscopy. These contrast agents are encapsulating microspheres with liquid-filled cores and various scattering particles incorporated into the protein shell, the core, or both. The flexible fabrication protocol for these agents allows for control of size, shell material, core material, and shell surface modifications. Further investigations will include modeling and optimizing the contrast agent's signal enhancement by varying microsphere size and by incorporating and encapsulating other combinations of scattering, absorbing, or light-modulating particles. A theoretical framework with which to predict the scattering properties of these contrast agents will need to account for the interaction between the host microsphere and the nanoparticles incorporated into its shell. Related research with multiple multipole expansions of the electromagnetic field suggests that one must also take into account the fractal nature of the distribution of nanoparticles.[13] Shell surface modifications will be used to target agents to specific tissue types such as neoplastic tissue. Similarly to contrast agents in other imaging modalities, these agents have the potential to increase the diagnostic utility of OCT by site-specifically targeting cells and tissues, particularly when pathological tissue is morphologically or optically similar to normal tissue.

We thank John Fahrner for his technical contributions and acknowledge the support of this research by the Whitaker Foundation (for S. A. Boppart) and the National Institutes of Health (grant HL25934 to K. S. Suslick). Additional information can be found at http://nb.beckman.uiuc.edu/biophotonics. S. A. Boppart's e-mail address is boppart@uiuc.edu.

References

1. C. Christiansen, H. Kryvi, P. C. Sontum, and T. Skotland, Biotechnol. Appl. Biochem. **19,** 307 (1994).
2. G. S. Gazelle, G. L. Wolf, G. L. McIntire, E. R. Bacon, E. F. Halpern, E. R. Cooper, and J. L. Torner, Acad. Radiol. **1,** 373 (1994).
3. M. Y. Su, A. Muhler, X. Lao, and O. Nalcioglu, Magn. Reson. Med. **39,** 259 (1998).
4. J. E. Bugaj, S. Achilefu, R. B. Dorshow, and R. Rajagopalan, J. Biomed. Opt. **6,** 122 (2001).
5. B. E. Bouma and G. J. Tearney, eds., *Handbook of Optical Coherence Tomography* (Marcel Dekker, New York, 2001).
6. K. J. Liu, M. W. Grinstaff, J. Jiang, K. S. Suslick, H. M. Swartz, and W. Wang, Biophys. J. **67,** 896 (1994).
7. S. A. Boppart, B. E. Bouma, C. Pitris, J. F. Southern, M. E. Brezinski, and J. G. Fujimoto, Nature Med. **4,** 861 (1998).
8. J. K. Barton, J. B. Hoying, and C. J. Sullivan, Acad. Radiol. **9S,** 52 (2002).
9. A. Vitkin, J. Woolsey, B. C. Wilson, and R. R. Anderson, Photochem. Photobiol. **59,** 455 (1994).
10. S. K. Kurtz, S. D. Kozikowski, and L. J. Wolfram, in *Electro-Optics and Photorefractive Materials*, P. Gunther, ed. (Springer-Verlag, Berlin, 1986), p. 110.
11. L. Wang and S. L. Jacques, Appl. Opt. **34,** 2362 (1995).
12. D. L. Marks, A. L. Oldenburg, J. J. Reynolds, and S. A. Boppart, Opt. Lett. **27,** 2010 (2002).
13. K. A. Fuller, J. Opt. Soc. Am. A **12,** 881 (1995).